

A Step Toward an NIR-Emitting ESIPT Probe for Smart Zn²⁺ Sensing in Different Environments

Junfeng Wang, Yingbo Li, and Yi Pang*

Cite This: *Chem. Biomed. Imaging* 2023, 1, 537–540

Read Online

ACCESS |

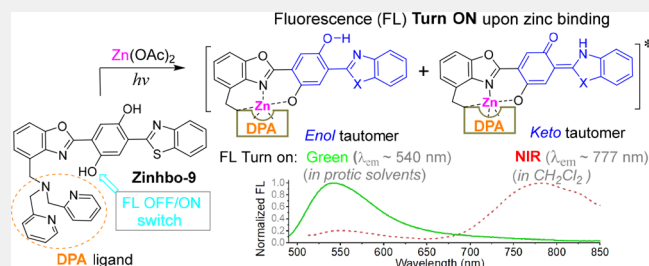
Metrics & More

Article Recommendations

Supporting Information

ABSTRACT: Current sensors for Zn²⁺ detection are largely based on the photoinduced electron transfer (PET) mechanism, which can effectively change the fluorescence intensity, without inducing a significant spectral shift. By coupling the PET mechanism with an excited state intramolecular proton transfer (ESIPT), a near-infrared fluorescent sensor was developed for Zn²⁺ detection. Upon binding to the Zn²⁺ cation, the sensor was able to generate *two* well-separated emission bands ($\lambda_{em} \approx 540$ and 770 nm), whose ratio was quite sensitive to the probe's environments. The finding offers an advanced tool for *in vitro* and *in vivo* imaging of the Zn²⁺ cation, which is desirable for future discovery of the biological functions of zinc.

KEYWORDS: fluorescent probe, zinc sensing, near-infrared emission, proton transfer, environmental sensitivity, fluorescence imaging

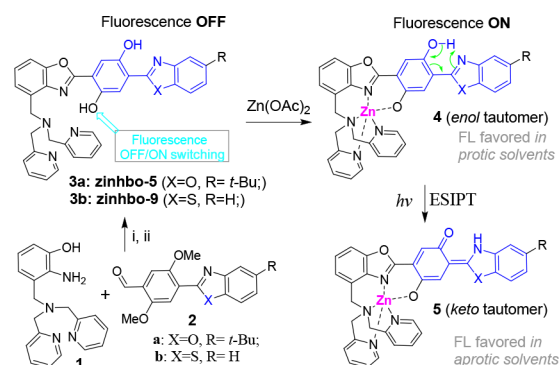


Molecular imaging is widely used to visualize the fundamental biological processes.^{1–3} Due to its high sensitivity, quick response, and excellent spatial and temporal resolution, fluorescent sensing has become one of the top choices to detect the analytes of interest.^{4,5} Near-infrared (NIR) fluorescent sensors are especially attractive for *in vivo* detection of biologically relevant species,^{6,7} as the NIR photon has deep tissue penetration and low autofluorescence.^{8–16} For applications, the emission should be well-separated from the excitation (i.e., large Stokes' shift), in order to minimize the interference from the excitation light.^{17–19} Although cyanine-based dyes give strong NIR absorption and emission, they exhibit small Stokes' shifts (usually 20–50 nm).^{19–24} Development of NIR fluorescent dyes with a large Stokes' shift (e.g., >200 nm) remains a challenge.

As an active component in enzymes and proteins,^{25–27} the zinc cation (Zn²⁺) plays an important role in various biological²⁸ and pathological processes, including Alzheimer's disease, epilepsy, infantile diarrhea, and ischemic stroke.^{29–33} Free zinc pools exist in some tissues, such as the brain, intestines, pancreas, and retina.³⁴ There is significant interest in sensing Zn²⁺ in living systems.^{35–42} However, the majority of Zn²⁺ sensors give emissions in the visible region, which often suffer interference from autofluorescence.⁴³ Most zinc sensors are based on the photoinduced electron transfer (PET) mechanism,^{35,44} which can induce a large fluorescence change. It should be noticed that metal ion binding typically induces a small spectral shift.^{44,45} In addition, PET often exhibits incomplete fluorescence quenching that limits the performance of the sensors. Solving the problem requires integration of other mechanisms in the sensor design.

In order to overcome the deficiency of PET-based sensors, a potential solution is based on a bis(HBO) 3 (Scheme 1). In the central phenyl ring of 3, one –OH group acts as a fluorescence OFF/ON switch when it binds to the Zn²⁺ cation. The second –OH group in 3 is reserved for the excited state intramolecular proton transfer (ESIPT) that can trigger a large

Scheme 1. Convergent Synthesis of Zinhbo-9^a



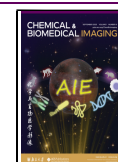
^aConditions: (i) xylenes 120 °C, O₂/activated carbon, 48 h, 52%; (ii) BBr₃, DCM, –78 °C to rt; overnight, 87%.

Received: March 22, 2023

Revised: April 15, 2023

Accepted: May 3, 2023

Published: May 17, 2023



spectral shift. The probe design utilizes Zn^{2+} binding to the $-\text{OH}$ switching group, thereby turning on the fluorescence of the ESIPT fluorophore, which can give two fluorescence signals.

Our recent studies showed that Zinhbo-5 (i.e., **3a** in Scheme 1) could be a useful NIR probe, as its binding to the Zn^{2+} cation can induce two fluorescence signals at ~ 540 and ~ 730 nm (in $\sim 1:1$ ratio), attributed to its enol and keto tautomers (Figure 1).⁴⁶ However, all the known bis(HBO) probes still

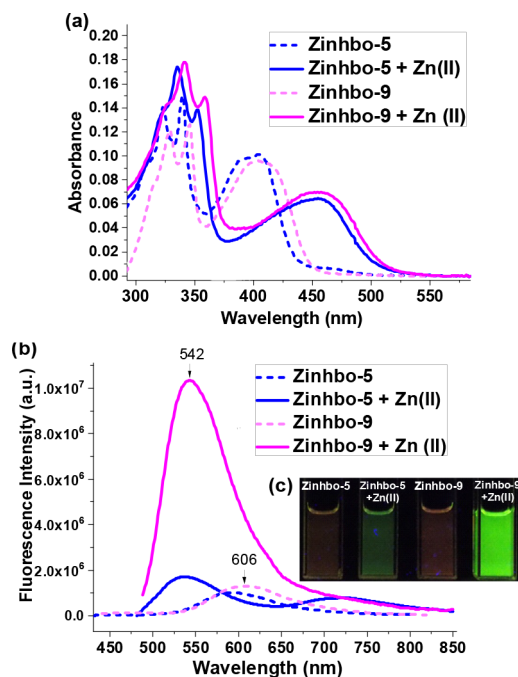


Figure 1. UV-vis (a) and fluorescence spectra (b) of $10 \mu\text{M}$ Zinhbo-5 and Zinhbo-9 (broken line) in aqueous solution containing 50% EtOH and their zinc complex (solid line). (c) Fluorescent images taken when the same samples (for spectra) were irradiated with a 365 nm UV lamp at room temperature.

exhibited relatively low NIR response upon Zn^{2+} binding, despite the efforts for over a decade.^{46,47} Herein, we demonstrate that the probe's response to Zn^{2+} could be dramatically improved by using Zinhbo-9 (**3b**), giving strong green ($\lambda_{\text{em}} \approx 540$ nm) or NIR fluorescence ($\lambda_{\text{em}} \approx 750\text{--}780$ nm), depending on the environments. The large NIR fluorescence turn on, in addition to its potential to sense its environment change, makes the probe a very attractive candidate for Zn^{2+} sensing.

Sensor Zinhbo-9 was synthesized in good yield by coupling the key intermediate aminophenol **1** with aldehyde **2b** in two steps (Scheme S1) using a convergent synthetic strategy.⁴⁸ UV-vis of Zinhbo-9 exhibited an absorption of $\lambda_{\text{max}} \approx 405$ nm, which was red-shifted to $\lambda_{\text{max}} \approx 455$ nm upon addition of the Zn^{2+} cation (Figure 1a, solid lines), indicating the complex formation. On the basis of the Job plot and ESI-MS data (Figure S1), the complex structure was assumed to be **4b** with a 1:1 ligand-to-metal ratio (i.e., Zinhbo-9/ Zn , Figure S2), which is consistent with the reported crystal structure for **4a**.⁴⁶ In the aqueous solution (EtOH: H_2O = 1:1), Zinhbo-9 alone gave a relatively weak fluorescence ($\lambda_{\text{em}} \approx 600$ nm, $\phi_{\text{fl}} \approx 0.11$ by using quinine sulfate as a reference). However, formation of the zinc complex drastically increased the fluorescence when being excited at 455 nm to give bright green emission ($\lambda_{\text{em}} \approx$

542 nm; $\phi_{\text{fl}} \approx 0.72$; Figure 1b,c). Although both ligands exhibited similar emission profile with $\lambda_{\text{em}} \approx 600$ nm, the zinc complex of Zinhbo-9 gave one bright emission peak ($\lambda_{\text{em}} \approx 542$ nm), while that of Zinhbo-5 gave two weak emission peaks ($\lambda_{\text{em}} \approx 540$ and 725 nm) in about a 1:1 ratio (Figure 1b). The large difference in responding to the Zn^{2+} cation indicated the large impact of a heteroatom substitution on the ESIPT process, as Zinhbo-9/ Zn in the aqueous buffer gave nearly exclusive emission from its enol tautomer.

The fluorescence of the new probe was further examined in different solvents (Figure S3). Interestingly, Zinhbo-9/ Zn gave mainly an enol emission ($\lambda_{\text{em}} \sim 540$ nm) in a protic solvent such as EtOH. The enhanced enol emission from Zinhbo-9/ Zn in a protic solvent was in sharp contrast to that from Zinhbo-5/ Zn , whose ESIPT emission (from the keto tautomer) was enhanced in EtOH (Figures S4–S6). It was assumed that the hydrogen bonding with protic solvents inhibited the ESIPT process effectively in Zinhbo-9/ Zn , making it possible to achieve a predominant enol emission.

More interestingly, Zinhbo-9/ Zn exhibited a major NIR emission peak at ~ 770 nm in CH_2Cl_2 and dual emission ($\lambda_{\text{em}} \approx 534$ and 770 nm in about 1:1 ratio) in CH_3CN , showing that the emission of the zinc complex was quite sensitive to its environments (Figure 2 and Figure S3). The NIR emission

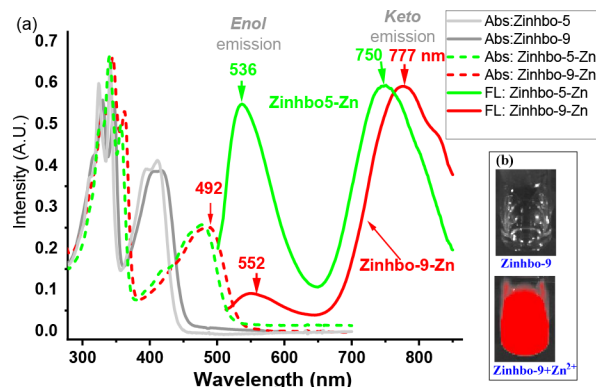


Figure 2. (a) Normalized absorption (ABS) and fluorescence (FL) spectra of Zinhbo-5 and Zinhbo-9 upon addition of 1.0 equiv of Zn^{2+} in CH_2Cl_2 excited at λ_{max} (480 and 492 nm). (b) Zinhbo-9 and Zinhbo-9/ Zn^{2+} CH_2Cl_2 solution ($1.0 \mu\text{M}$) in glass scintillation vials were imaged with Ex/Em = 500/780 nm (NIR channel) using an IVIS imaging system.

peak at ~ 770 nm could be attributed to its keto tautomer **5**. The result thus illustrated a rare probe that gave strong NIR emission with a very large Stokes' shift ($\Delta\lambda = (777 - 492)$ nm = 285 nm) upon binding to Zn^{2+} by selectively turning on its keto emission in an aprotic solvent. In addition, the emission ratio of the resulting Zn^{2+} complex at 534 and 770 nm was quite sensitive to its environment. Thus, the NIR-emitting new probe not only is capable of detecting zinc cation but also raising the possibility of detecting zinc in different bioenvironments. The Zn^{2+} binding induced NIR emission can be clearly observed by using an "in vivo imaging spectrum (IVIS)" system (Figure 2B).

The apparent association constant, $K_a = 6.41$ nM, for Zn^{2+} was determined, which reveals strong binding of Zinhbo-9 toward the Zn^{2+} cation, and the detection limit was found to be as low as 0.5 nM in the buffered aqueous (Figure S2S).

The sensor's response to other metal ions was also examined in both CH_2Cl_2 and aqueous solutions (Figures S9–S11). The probe was silent to other physiologically important metal ions, such as Mg^{2+} , Na^+ , and K^+ cations. The heavy and transition metal ions, such as Mn^{2+} , Ni^{2+} , Co^{2+} , Cu^{2+} , Fe^{2+} , Fe^{3+} , Pb^{2+} , Ba^{2+} , and Cr^{3+} cations, which are well-known fluorescence quenchers, did not show a fluorescence quenching effect on Zinhbo-9 in both CH_2Cl_2 and aqueous solutions. Furthermore, significant fluorescence turn-on was observed in the presence of 10 equiv of the other metal ion and 1 equiv of Zn^{2+} in aqueous solution, which indicates that all the tested metal ions did not interfere with Zn^{2+} sensing. Therefore, Zinhbo-9 is a highly selective NIR fluorescence turn-on chemosensor for the Zn^{2+} cation.

For Zn^{2+} sensing, a significant challenge is to differentiate Zn^{2+} from Cd^{2+} , as both cations have similar electron configuration. Interestingly, Zinhbo-9 did not exhibit notable change in absorption, λ_{max} upon binding Cd^{2+} in CH_2Cl_2 , and the resulting Cd^{2+} complex did not give NIR emission (Figures S12–S15). The dissociation constant using the Benesi–Hildebrand plot revealed that Zinhbo-9 exhibited stronger binding toward Zn^{2+} [e.g., $K_{\text{d}} \approx 17.9 \mu\text{M}$ for Zn^{2+} and $K_{\text{d}} \approx 86.0 \mu\text{M}$ for Cd^{2+} in CH_2Cl_2 (Figure S17)]. The competitive binding of the probe toward Zn^{2+} and Cd^{2+} was also examined in HEPES buffer (Figures S22–S26), revealing the same trend. Replacement of Cd^{2+} by Zn^{2+} in the preformed Zinhbo-9/ Cd^{2+} complex solution was observed, which further indicated the stronger binding of Zn^{2+} over Cd^{2+} . Therefore, Zinhbo-9 provided a rare NIR sensor that can selectively detect the Zn^{2+} cation.

In order to examine its biological applications, the probe was applied to cells by staining human mesenchymal stem cells (hMSCs). When the samples were excited with a 488 nm laser, strong NIR fluorescence (700–800 nm) was observed from the intracellular area (Figure S26), and only a very weak signal was observed in the green channel. In a control experiment, negligible intracellular fluorescence was detected from the cells after being treated with $10 \mu\text{M}$ Zinhbo-9 for 60 min (Figure S26c). The weak signal observed in the control experiment was attributed to the natural presence of an endogenous zinc cation. These results demonstrated that the probe could be a suitable tool for determining intracellular Zn^{2+} activities. An interesting feature is that Zinhbo-9 appeared to pass through the karyotheca (or nuclear membrane) into the nuclei, which was quite different from that of Zinhbo-5 (mainly spreads in the cytoplasm).⁴⁹ To further confirm this feature, Zinhbo-9 was applied to a more divisive cell line (HeLa cells) with a shortened staining time (Figure 3). A strong NIR signal was observed in nuclei, which further proved the nuclear staining by Zinhbo-9. Interestingly, the chromosomes were found to be brighter in the metaphase during mitosis, which indicates that zinc plays an important role in cell proliferation where an advanced zinc probe would be a useful tool.⁵⁰

It should be noted that the emission of the Zinhbo-9/ Zn complex was quite sensitive to the probe's environment (Figures 1 and 2). The strong NIR emission, coupled with very weak green emission, indicated that the Zinhbo-9/ Zn complex was located in a hydrophobic cellular or tissue environment. In other words, the comparison of zinc binding patterns from the green and NIR signals could provide useful information about the local environment of Zn^{2+} (i.e., aqueous or hydrophobic environments), which the existing zinc probes cannot match.

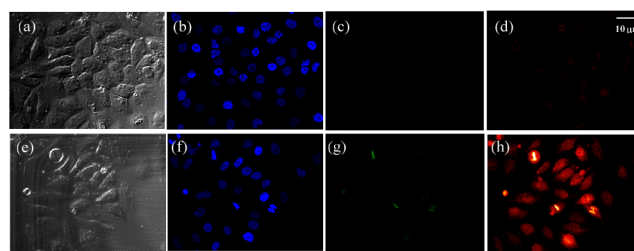


Figure 3. Confocal fluorescence images of HeLa cells excited with a 488 nm laser. The images were collected at bright field (a,e), DAPI (b,f), green channel (c,g), and NIR channel (d,h: 700–800 nm). Top (control): Cells were incubated with Zinhbo-9 for 60 min at 37°C in Dulbecco's modified Eagle's medium (DMEM). Bottom: Cells were first treated with Zn^{2+} ($10 \mu\text{M}$) for 30 min and further exposed to Zinhbo-9 ($10 \mu\text{M}$) for another 60 min at 37°C in DMEM.

Encouraged by the cell studies, we further investigated the potential of using Zinhbo-9 for in vivo imaging of zinc in a mouse model. The injection of Zinhbo-9 followed by further injection of a zinc ion generated strong NIR fluorescence. Mice treated only with the probe showed weaker NIR fluorescence under the same imaging conditions (Figure 4). In the control

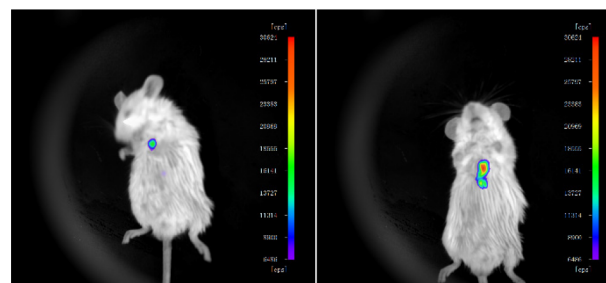


Figure 4. Fluorescent images of living mice. Left: Subcutaneous injection of $25 \mu\text{L}$ solution Zinhbo-9 (10 mM in DMSO). Right: Subcutaneous injection of $25 \mu\text{L}$ solution Zinhbo-9 (10 mM in DMSO), and then subcutaneous injection of $30 \mu\text{L}$ of Zn^{2+} solution ($10 \mu\text{M}$ in DMSO). Images were taken 20 min after the subcutaneous injection, with Ex/Em = 500/780 nm (NIR channel) using an IVIS imaging system.

experiment, the NIR fluorescent signal around the injection site might derive from the tissue injury, which has been known to cause dramatic elevation of zinc.⁵¹ These results demonstrate that the Zinhbo-9 probe is a useful Zn^{2+} -selective NIR probe for in vivo fluorescence imaging.

In addition, the Zinhbo-9/ Zn complex also exhibited significant fluorescence at 777 nm when being excited at 980 nm in CH_2Cl_2 (Figures S6 and S7). The probe thus could have both excitation and emission within the NIR-I region (700–1000 nm), an ideal feature for an NIR sensor.

In conclusion, Zinhbo-9 has been shown to be a highly selective fluorescent turn-on sensor for Zn^{2+} cations, giving NIR emission at $\sim 777 \text{ nm}$. The finding leads to a promising molecular design which allows the probe to generate NIR emission ($\lambda_{\text{em}} \approx 777 \text{ nm}$) that is well-separated from its excitation ($\lambda_{\text{max}} \approx 492 \text{ nm}$). In addition, the formed zinc complex Zinhbo-9/ Zn exhibited attractive environmental sensing properties, giving emission at two drastically different wavelengths (i.e., 540 nm for protic and 770 nm for nonpolar environments). Use of the probe in cancer cells and stem cells further demonstrates its potential for biological applications.

Since Zinhbo-9 possesses many desirable features that the current zinc sensors cannot match, the developed sensor could be of practical importance for future biological research.

■ ASSOCIATED CONTENT

SI Supporting Information

The Supporting Information is available free of charge at <https://pubs.acs.org/doi/10.1021/cbmi.3c00037>.

Full experimental details, characterization data of all new compounds, spectroscopic assay conditions, and in vitro and in vivo experimental conditions (PDF)

■ AUTHOR INFORMATION

Corresponding Author

Yi Pang – Department of Chemistry & Maurice Morton Institute of Polymer Science, The University of Akron, Akron, Ohio 44325, United States; orcid.org/0000-0001-7275-4563; Email: yp5@uakron.edu

Authors

Junfeng Wang – Department of Chemistry & Maurice Morton Institute of Polymer Science, The University of Akron, Akron, Ohio 44325, United States; Gordon Center for Medical Imaging, Massachusetts General Hospital and Harvard Medical School, Boston, Massachusetts 02114, United States
Yingbo Li – State Key Laboratory of Natural and Biomimetic Drugs, School of Pharmaceutical Sciences, Peking University, Beijing 100191, China

Complete contact information is available at: <https://pubs.acs.org/10.1021/cbmi.3c00037>

Notes

The authors declare no competing financial interest.

■ ACKNOWLEDGMENTS

Y.P. acknowledges the support of the Coleman endowment from the University of Akron.

■ REFERENCES

- (1) Lichtman, J. W.; Conchello, J. A. *Nat. Methods* **2005**, *2*, 910–19.
- (2) Loudet, A.; Burgess, K. *Chem. Rev.* **2007**, *107*, 4891–932.
- (3) Goncalves, M. S. T. *Chem. Rev.* **2009**, *109*, 190–212.
- (4) Boens, N.; Leen, V.; Dehaen, W. *Chem. Soc. Rev.* **2012**, *41*, 1130–72.
- (5) Yang, Y.; Cheng, T.; Zhu, W.; Xu, Y.; Qian, X. *Org. Lett.* **2011**, *13*, 264–7.
- (6) Yuan, L.; Lin, W.; Zheng, K.; He, L.; Huang, W. *Chem. Soc. Rev.* **2013**, *42*, 622–61.
- (7) Klohs, J.; Wunder, A.; Licha, K. *Basic Research in Cardiology* **2008**, *103*, 144–51.
- (8) Weissleder, R. *Nat. Biotechnol.* **2001**, *19*, 316–7.
- (9) Frangioni, J. V. *Curr. Opin. Chem. Biol.* **2003**, *7*, 626–34.
- (10) Hilderbrand, S. A.; Weissleder, R. *Curr. Opin. Chem. Biol.* **2010**, *14*, 71–9.
- (11) Escobedo, J. O.; Rusin, O.; Lim, S.; Strongin, R. M. *Curr. Opin. Chem. Biol.* **2010**, *14*, 64–70.
- (12) Oushiki, D.; Kojima, H.; Terai, T.; Arita, M.; Hanaoka, K.; Urano, Y.; Nagano, T. *J. Am. Chem. Soc.* **2010**, *132*, 2795–801.
- (13) Karton-Lifshin, N.; Segal, E.; Omer, L.; Portnoy, M.; Satchi-Fainaro, R.; Shabat, D. *J. Am. Chem. Soc.* **2011**, *133*, 10960–5.
- (14) Yuan, L.; Lin, W. Y.; Zhao, S.; Gao, W. S.; Chen, B.; He, L. W.; Zhu, S. S. *J. Am. Chem. Soc.* **2012**, *134*, 13510–23.
- (15) Hawrysz, D. J.; Sevick-Muraca, E. M. *Neoplasia* **2000**, *2*, 388–417.
- (16) Kobayashi, H.; Ogawa, M.; Alford, R.; Choyke, P. L.; Urano, Y. *Chem. Rev.* **2010**, *110*, 2620–40.
- (17) Peng, X.; Song, F.; Lu, E.; Wang, Y.; Zhou, W.; Fan, J.; Gao, Y. *J. Am. Chem. Soc.* **2005**, *127*, 4170–1.
- (18) Zhang, Z.; Achilefu, S. *Org. Lett.* **2004**, *6*, 2067–70.
- (19) Tolosa, L.; Nowaczyk, K.; Lakowicz, J. *An Introduction to Laser Spectroscopy*, 2nd ed.; Kluwer: New York, 2002.
- (20) Goncalves, M. S. T. *Chem. Rev.* **2009**, *109*, 190–212.
- (21) Sasaki, E.; Kojima, H.; Nishimatsu, H.; Urano, Y.; Kikuchi, K.; Hirata, Y.; Nagano, T. *J. Am. Chem. Soc.* **2005**, *127*, 3684–5.
- (22) Kiyose, K.; Kojima, H.; Urano, Y.; Nagano, T. *J. Am. Chem. Soc.* **2006**, *128*, 6548–9.
- (23) Tang, B.; Yu, F.; Li, P.; Tong, L.; Duan, X.; Xie, T.; Wang, X. *J. Am. Chem. Soc.* **2009**, *131*, 3016–23.
- (24) Weissleder, R.; Ntziachristos, V. *Nat. Med.* **2003**, *9*, 123–8.
- (25) Jiang, P.; Guo, Z. *Coord. Chem. Rev.* **2004**, *248*, 205–29.
- (26) Outten, C. E.; O'Halloran, T. V. *Science* **2001**, *292*, 2488–92.
- (27) Finney, L. A.; O'Halloran, T. V. *Science* **2003**, *300*, 931–6.
- (28) Berg, J. M.; Shi, Y. *Science* **1996**, *271*, 1081–5.
- (29) Bush, A. I.; Pettingell, W. H.; Multhaup, G.; Paradis, M.; Vonsattel, J.-P.; Gusella, J. F.; Beyreuther, K.; Masters, C. L.; Tanzi, R. E. *Science* **1994**, *265*, 1464–7.
- (30) Koh, J. Y.; Suh, S. W.; Gwag, B. J.; He, Y. Y.; Hsu, C. Y.; Choi, D. W. *Science* **1996**, *272*, 1013–6.
- (31) Frederickson, C. J.; Hernandez, M. D.; McGinty, J. F. *Brain Res.* **1989**, *480*, 317–21.
- (32) Walker, C. F.; Black, R. E. *Annu. Rev. Nutr.* **2004**, *24*, 255–75.
- (33) Lee, J.-Y.; Cole, T. B.; Palmiter, R. D.; Suh, S. W.; Koh, J. Y. *Proc. Natl. Acad. Sci. U. S. A.* **2002**, *99*, 7705–10.
- (34) Xu, Z. C.; Yoon, J. Y.; Spring, D. R. *Chem. Soc. Rev.* **2010**, *39*, 1996–2006.
- (35) Nolan, E. M.; Lippard, S. J. *Acc. Chem. Res.* **2009**, *42*, 193–203.
- (36) Carol, P.; Sreejith, S.; Ajayaghosh, A. *Chem.-Asian J.* **2007**, *2*, 338–48.
- (37) Pluth, M. D.; Tomat, E.; Lippard, S. J. *Annu. Rev. Biochem.* **2011**, *80*, 333–355.
- (38) Zhang, J.; Peng, X.; Wu, Y.; Ren, H.; Sun, J.; Tong, S.; Liu, T.; Zhao, Y.; Wang, S.; Tang, C.; Chen, L.; Chen, Z. *Angew. Chem., Int. Ed.* **2021**, *60*, 25846–25855.
- (39) Fang, H.; Geng, S.; Hao, M.; Chen, Q.; Liu, M.; Liu, C.; Tian, Z.; Wang, C.; Takebe, T.; Guan, J. L.; Chen, Y.; Guo, Z.; He, W.; Diao, J. *Nat. Commun.* **2021**, *12*, 109.
- (40) Feng, J.; Li, J.-Z.; Mao, X.-M.; Wang, Q.; Li, S.-P.; Wang, C.-Y. *Analyst* **2021**, *146*, 3971–3976.
- (41) Liu, R.; Kowada, T.; Du, Y.; Amagai, Y.; Matsui, T.; Inaba, K.; Mizukami, S. *ACS Sens.* **2022**, *7*, 748–757.
- (42) Fang, F.; Chen, Y.; Jiang, Z.; He, W.; Guo, Z. *Acc. Chem. Res.* **2023**, *56*, 258–269.
- (43) You, Y.; Lee, S.; Kim, T.; Ohkubo, K.; Chae, W.-S.; Fukuzumi, S.; Jhon, G.-J.; Nam, W.; Lippard, S. J. *J. Am. Chem. Soc.* **2011**, *133*, 18328–42.
- (44) Carter, K. P.; Young, A. M.; Palmer, A. E. Fluorescent Sensors for Measuring Metal Ions in Living Systems. *Chem. Rev.* **2014**, *114*, 4564–4601.
- (45) Kiyose, K.; Kojima, H.; Urano, Y.; Nagano, T. *J. Am. Chem. Soc.* **2006**, *128*, 6548–9.
- (46) Xu, Y.; Liu, Q.; Dou, B.; Wright, B.; Wang, J.; Pang, Y. *Adv. Healthcare Mater.* **2012**, *1*, 485–92.
- (47) Xu, Y.; Pang, Y. *Chem. Commun.* **2010**, *46*, 4070–4072.
- (48) Wang, J. F.; Pang, Y. *RSC Adv.* **2013**, *3*, 10208–12.
- (49) Wang, J. F.; Baumann, H.; Bi, X.; Shriver, L. P.; Zhang, Z.; Pang, Y. *Bioorganic Chemistry* **2020**, *96*, 103585.
- (50) Beyersmann, D.; Haase, H. *BioMetals* **2001**, *14*, 331–341.
- (51) Sharir, H.; Zinger, A.; Nevo, A.; Sekler, I.; Hershfinkel, M. J. *Biol. Chem.* **2010**, *285*, 26097–26106.